

An Internal Standardisation Strategy for Quantitative Immunoassay Tissue Imaging using Laser Ablation Inductively Coupled Plasma Mass Spectrometry

Daniel A. Frick^a, Charlotte Giesen^b, Teresa Hemmerle^c, Bernd Bodenmiller^b, Detlef Günther^{a*}

^aDepartment of Chemistry and Applied Biosciences, Laboratory of Inorganic Chemistry, ETH Zürich, Zürich, Switzerland, *E-mail: guenther@inorg.chem.ethz.ch

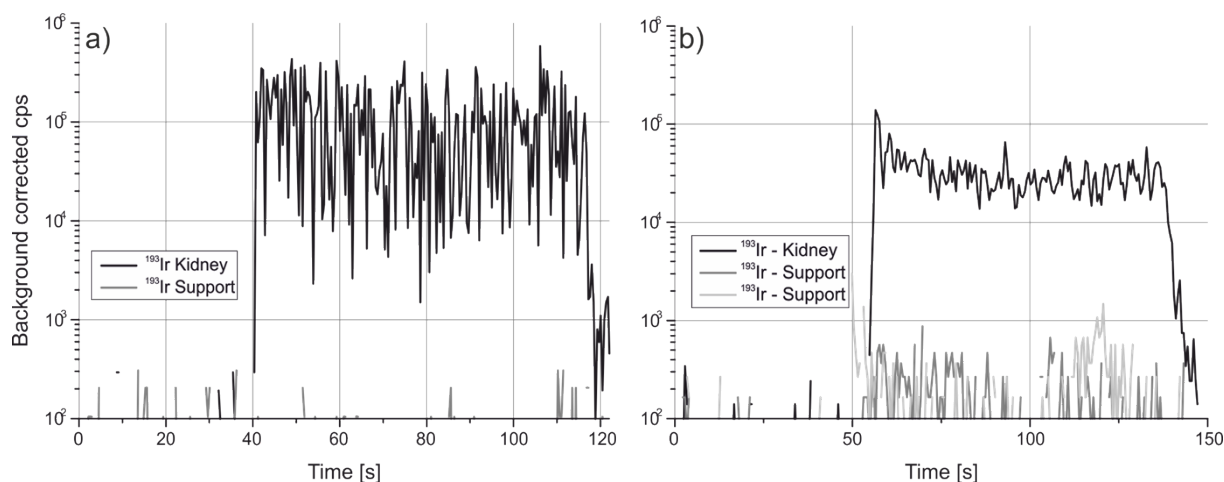
^bInstitute of Molecular Life Sciences, University of Zürich, Zürich, Switzerland

^cDepartment of Chemistry and Applied Biosciences, Institute of Pharmaceutical Sciences, ETH Zürich, Zürich, Switzerland

Supporting Information

Background contamination

Supplementary Figure 1 shows the background contamination of iridium next to the tissue samples for a) paraffin imbedded tissue sections and b) for the cryo sections. Whereas for the FFPE section the iridium signal intensities are on background level, the cryo sections show elevated count rates (≈ 200 cps) compared to the gas blank (≈ 30 cps) indicating a cross contamination of the embedding cryo medium.



Supplementary Figure 1: Background corrected signal intensities for ^{193}Ir for a) paraffin imbedded tissue and b) for cryo-cut tissue. Contamination of the support with the internal standard was smaller when applied to the paraffin thin sections compared to the cryo thin section. Possible explanation is residue of the cryo medium which was not entirely removed.

Standard cryo sections preparation from liver cells

A liver of a Balb/c mouse (Elevage Janvier) was comminuted and pressed through a $40\ \mu\text{m}$ nylon sieve (Nunc). Red blood cells were lysated and liver cells separated from supernatant by centrifugation. The cells were dispersed in 5 mL of a multi-element solution containing REE and iridium and incubated 10 minutes on ice on a horizontal shaker. The multi-element solution was prepared directly prior from single element standard solution diluted in ultrapure water (no nitric acid was added). After a centrifugation step, the cell pellet was frozen in liquid nitrogen, embedded as for the whole organ cryo sections, cut and stored at $-80\ ^\circ\text{C}$.

The cryo sections were fixed for 10 minutes in -20 °C cold acetone (p.a.) and stored at RT until ablation. Part of the cell pellet was analysed using microwave assisted digestion and SN-ICP-MS with an external calibration to determining the concentration of iridium.

LA-ICP-MS

Laser ablation experiments were carried out on an ArF excimer-based UV-LA (193 nm) (GeoLasC, MicroLas Lasersystem GmbH, Göttingen, Germany) unit equipped with a computer controlled xyz-stage, petrographic microscope (Olympus BX-51, Olympus Schweiz AG, Volketswil, Switzerland) and camera (HV-D20, Hitachi Kokusai Electric Inc., Tokyo, Japan) for the simultaneous observation of the samples. The energy of the laser was adjusted such that the underlying support material was not ablated. The samples were ablated typically with a 24 µm spot, in raster mode with 24 µm/s and 10 Hz ablation frequency. The LA operating conditions are summarized in Supplementary Table 1. The samples were either placed in a low dispersion, high capacity, laser ablation cell (LDHCLA cell)¹ or in a circular ablation cell². Helium was used as carrier gas (typically 1.2 L/min). The aerosol was mixed with Argon in front of the injector using a laminar flow adapter. The Element2 (Thermo Scientific, Bremen, Germany) was tuned daily to highest intensity, with a typical ²³²Th¹⁶O/²³²Th ratio of 0.01 and a ²³⁸U/²³²Th close to 1 determined on NIST SRM612 (National Institute of Standards and Technology, Gaithersburg, MD, USA). The instrument was operated in low mass resolution in speed acquisition mode with 1 Sample/Isotope with a dwell time of 10 ms.

Laser	GeoLas C
Crater size	24 µm
Scan speed	24 µm/s
Fluence	0.7 J/cm ²
Carrier gas type	Helium
Flow rate	1.2 L/min
ICP-MS	Element2
RF power	1280 W
Nebuliser flow	0.852 L/min
Auxiliary flow	0.82 L/min
Cool gas flow	16 L/min
Number of elements	8
Mass Window	10 %
Samples / Peak	10
Dwell time / Sample	10 ms
Replicates	355
Acquisition Mode	Speed

Supplementary Table 1: Laser ablation and ICP-MS settings used for the investigation of the background contamination, the thickness correlation and the imaging of the tissue samples.

High Spatial Resolution LA-ICP-MS

A part of the tissue was also analysed with a high spatial resolution LA-ICP-MS system.³ Due to the unique design of the ablation cell, the aerosol is entrained and transported very efficiently, single shots with up to 20-30 Hz can be temporally resolved. The LA operating conditions are summarized in *Supplementary Table 2*. The measurement using a crater size of 5 µm was performed on the Element2.

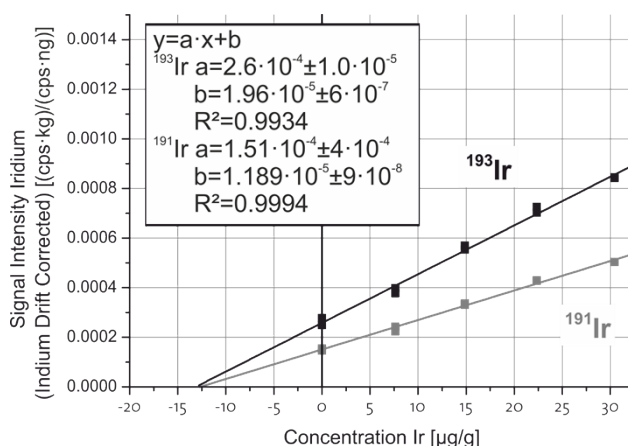
Laser	GeoLas C
Crater size	5 µm
Scan speed	10 µm/s
Frequency	10 HZ
Fluence	15 J/cm ²
Carrier gas type	Helium

Flow rate	0.9 L/min
ICP-MS	Element2
RF power	1280 W
Nebuliser flow	0.863 L/min
Auxiliary flow	0.83 L/min
Cool gas flow	16 L/min
Number of elements	6
Mass Window	10 %
Samples / Peak	50
Dwell time / Sample	2 ms
Replicates	400
Acquisition Mode	Speed

Supplementary Table 2: Laser ablation and ICP-MS settings used for the high spatial resolution LA-ICP-MS measurement.

Standard Addition

Supplementary Figure 2 shows the results of the standard addition to determine the concentration of the internal standard in the FFPE kidney section. Five solutions with increasing iridium concentration and constant indium concentration were aspirated while ablating a tissue section of constant thickness. Differences in sensitivity from laser generated and dried aerosol was determined on a liver cryo section with a known thickness and the concentration of iridium was determined by sn-ICP-MS after digestion.

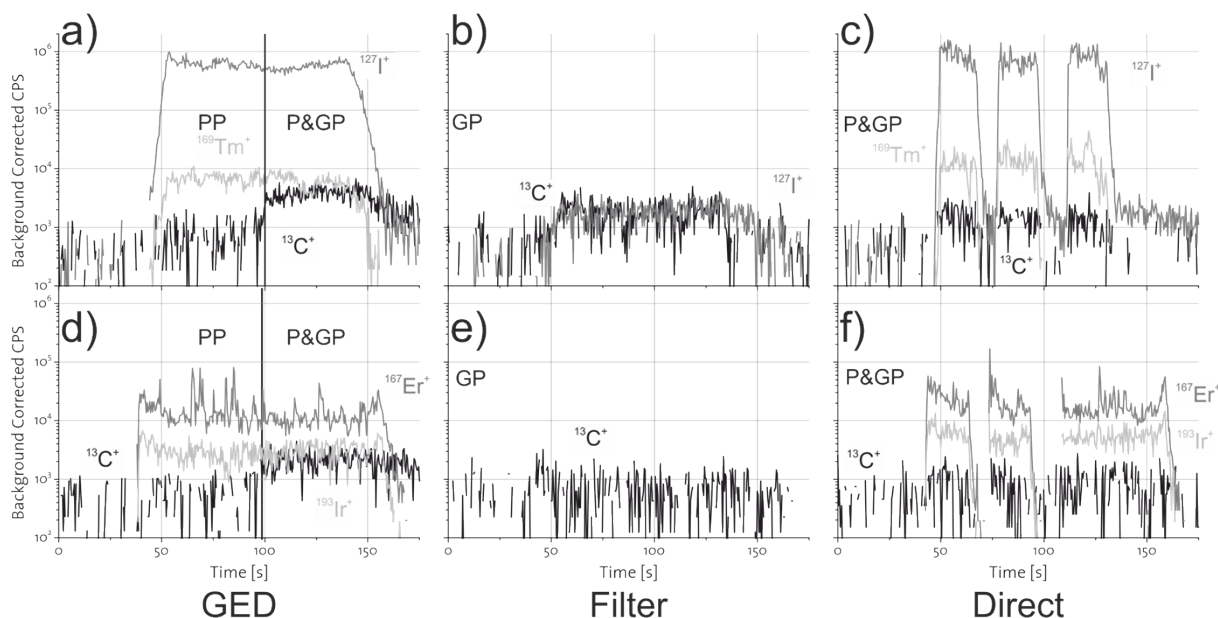


Supplementary Figure 2: Results of the standard addition to determine the concentration of the internal standard in the FFPE kidney section.

Gasphase formation on tissue samples

Similar to an earlier study about the carbon containing gas phase (CCGS) and carbon particulate phase (CPP)⁴ the formation of gaseous iodine and iridium species during the ablation of tissue samples was investigated. For this, two samples were ablated, first, a 10µm cryo kidney tissue also used in the correlation experiments and, second, a tonsil tissue sample (obtained from Charlotte Giesen, BAM) stained with iodine according to procedure described by Giesen *et al.*⁵ The samples were ablated under identical conditions with argon as a carrier gas. Supplementary Figure 3a and d) show the laser aerosol passing the gas exchange device (GED, which is based on a design described by Nishiguchi *et al.*⁶ and Kovacs *et al.*⁷). First the gas exchange is active, enabling only the particulate phase of the laser generated aerosol entering the plasma. In the second half the gas exchange is turned off and the particulate phase is entering the plasma together with the gas phase. Carbon forms a gaseous phase during the ablation for both samples, while the rare earth elements ($^{169}\text{Tm}^+$ and $^{167}\text{Er}^+$) are not affected by the gas exchange. Due to nature of the samples the homogeneity of the added analytes cannot be assumed and therefore a direct comparison between particulate phase and particulate & gas phase is not possible. Supplementary Figure 3b and e) show the gas phase which is able to pass the membrane

filters (0.4 μm pore size, Millipore, Billerica, MA, USA) showing a small part of iodine is penetrating the filters whereas the analytes ($^{169}\text{Tm}^+$ respectively $^{167}\text{Er}^+$) are retained on the filter. Supplementary Figure 3c and f) show the direct introduction of the laser aerosol with three distinct line scans showing that iodine tends to tail (see iodine signal in Supplementary Figure 3c) during the washout, whereas iridium washes out as the analytes.



Supplementary Figure 3: a-c) show the results from the iodine stained tonsil tissue sample and d-f) the kidney sample stained with the iridium intercalator. a) and d) show the laser aerosol passing the gas exchange device (GED), in the first part the GED is turned on and the gas phase are exchanged, a clear formation of a carbon containing gas phase is seen when the GED is turned off. b and e) show the laser aerosol passing a membrane filter. The analyte ($^{169}\text{Tm}^+$ respectively $^{167}\text{Er}^+$) are retained on the filters, whereas a small fraction of iodine is able to pass the membrane filter. Contrariwise iridium is on background level. c and f) show the direct introduction of the laser aerosol, iodine tends to have a longer tailing during the washout whereas iridium washes out as the analyte (in this case $^{167}\text{Er}^+$).

Literature

1. M. B. Fricker, D. Kutscher, B. Aeschlimann, J. Frommer, R. Dietiker, J. Bettmer and D. Günther, *Int. J. Mass Spectrom.*, 2011, **307**, 39-45. DOI: 10.1016/j.ijms.2011.01.008.
2. B. Hattendorf, Ph.D. Thesis NO. 14926, Eidgenössische Technische Hochschule Zürich, 2002.
3. H. A. O. Wang, D. Grolimund, C. Giesen, C. N. Borca, J. R. H. Shaw-Stewart, B. Bodenmiller and D. Günther, *Anal. Chem.*, 2013, **85**, 10107-10116. DOI: 10.1021/AC400996x.
4. D. A. Frick and D. Günther, *J. Anal. At. Spectrom.*, 2012, **27**, 1294-1303. DOI: 10.1039/C2ja30072a.
5. C. Giesen, L. Waentig, T. Mairinger, D. Drescher, J. Kneipp, P. H. Roos, U. Panne and N. Jakubowski, *J. Anal. At. Spectrom.*, 2011, **26**, 2160-2165. DOI: 10.1039/C1ja10227c.
6. K. Nishiguchi, K. Utani and E. Fujimori, *J. Anal. At. Spectrom.*, 2008, **23**, 1125-1129. DOI: 10.1039/b802302f.
7. R. Kovacs, K. Nishiguchi, K. Utani and D. Günther, *J. Anal. At. Spectrom.*, 2010, **25**, 142-147. DOI: 10.1039/b924425e.